

Photoexcitation and doping studies of poly(3-hexylthienylene)

Y. H. Kim, D. Spiegel, S. Hotta,* and A. J. Heeger

Department of Physics and Institute for Polymers and Organic Solids, University of California, Santa Barbara, Santa Barbara, California 93106

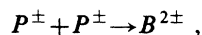
(Received 11 April 1988)

Comprehensive (0.05–3-eV) spectroscopic measurements are reported for poly(3-hexylthienylene), P3HT, during photoexcitation (i.e., photoinduced absorption) and after doping with NOPF₆. A one-to-one correspondence between the photoinduced and doping-induced spectral changes is observed, typical of conducting polymers. The results demonstrate that charges are predominantly stored in bipolarons in P3HT. We find two subgap electronic absorptions and a series of infrared-active vibrational (IRAV) modes. The four localized IRAV modes (1088, 1161, 1200, 1354 cm⁻¹) associated with bipolaron distortions of the P3HT chains and made infrared active through coupling to the uniform translation of the bipolaron were observed in both the doping-induced and photoinduced absorption spectra, as in polythiophene and poly(3-methylthienylene). An additional absorption (1396 cm⁻¹) was identified as arising from an ir-active localized mode associated with the nonuniform translation (shape oscillation) of the bipolaron. Comparison of the energies of the photoinduced and doping-induced electronic transitions yields an estimate of the change in Coulomb energy of the bipolaron on photoexcitation, $U_B \approx 0.25$ eV; this relatively small value of U_B is consistent with bipolaron formation in P3HT.

I. INTRODUCTION

Polythienylene (or polythiophene, PT) and the poly(3-alkylthienylene) derivatives are of interest as examples of a class of conjugated polymers in which the ground state is nondegenerate. The structure can be viewed (see Fig. 1) as analogous to *cis*-polyacetylene, but stabilized through the sulfur heteroatom which forms an aromatic ring. Because of the nondegenerate ground state, the important nonlinear excitations are polarons and bipolarons (confined soliton pairs).¹

Fundamentally important information about the nature of the nonlinear excitations in conjugated polymers can be obtained via photoexcitation (i.e., injecting charges onto the polymer backbone by direct optical pumping above the π - π^* energy gap with an intense external light source) and by charge transfer doping (chemically or electrochemical redox reaction with charge neutrality maintained through introduction of a counterion). Charge injection onto the backbone leads to local structural distortion and the formation of self-localized polarons or bipolarons with associated electronic states in the energy gap. For single charges, polarons (P^\pm) are formed; the reaction of pairs of polarons,



leads to bipolarons ($B^{2\pm}$). As a result, charged excitations cause characteristic new electronic transitions at energies in the gap at the expense of the oscillator strength of the interband transition.²

As a result of the distortion around the charge carrier, localized phonon modes (with enhanced infrared oscillator strength) are split off, one (or more) for each of the optical-phonon bands of the polymer. The photoinduced

infrared-active vibrational (IRAV) modes are therefore expected to be in one-to-one correspondence with the doping-induced IRAV, and both are expected to be in direct one-to-one correspondence with the Raman-active modes of the conjugated polymer.³ This can be understood in detail through the amplitude mode formalism,⁴ which accounts for the coupling of the lattice degrees of freedom to the uniform translational motion of the charged nonlinear excitation. Further detailed theoretical studies based on the Su-Schrieffer-Heeger (SSH) model¹ and its continuum version predicted two additional features: that an additional (but weaker) infrared-active localized mode should be expected (one for each Raman line) due to coupling to the shape oscillation (or nonuniform translational motion) of the charged nonlinear excitation;⁵ and that some weak infrared activity would be transferred to the extended phonon bands. Experimental evidence of the existence of both these weak modes and the extended phonon band⁶ have been reported for *trans*-polyacetylene,⁷ for PT and for P3MT.³

Doping and photoexcitation studies carried out on PT and on poly(3-methylthienylene), P3MT, have demonstrated that charge is stored predominantly in bipolarons; the doping-induced and photoinduced electronic transitions indicated the formation of two localized states in the gap associated with these charged excitations, and electron-spin-resonance measurements showed that the charged excitations are spinless.

Infrared photoexcitation absorption studies of PT and P3MT showed that the coupling strength of photogenerated charge carriers to ring deformations was less than 10% of the coupling to the translational degrees of freedom and thereby verified that the involvement of the heteroatom in the electronic structure of the thiophene ring is relatively weak.³ Therefore, a model which views

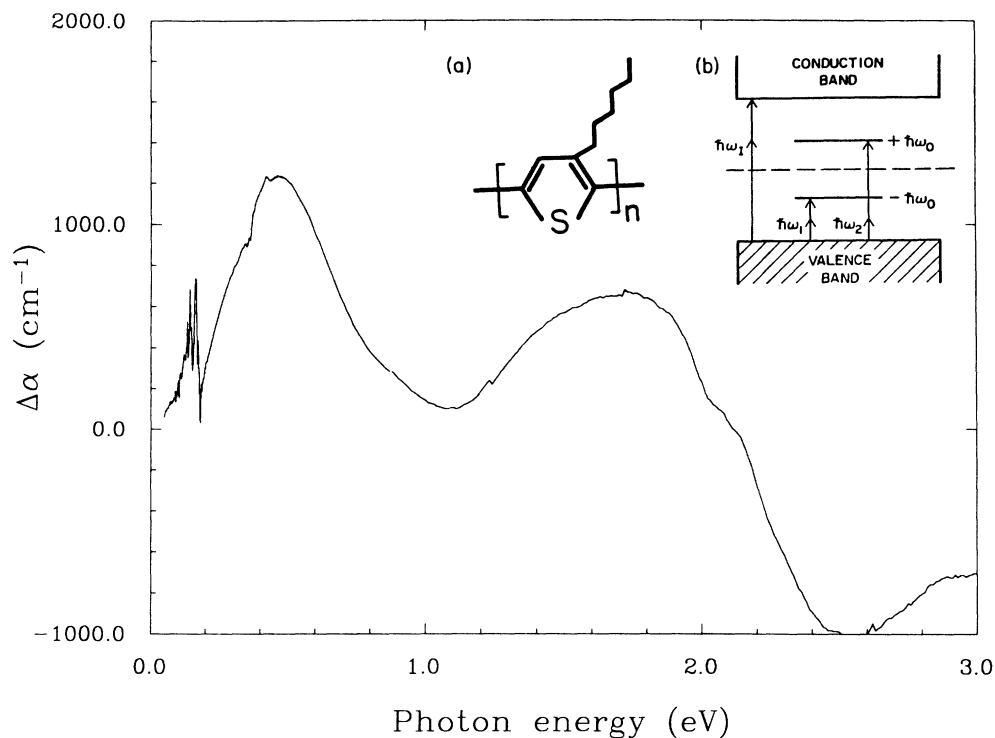


FIG. 1. Change in the absorption coefficient of P3HT after doping with 1 mol % of PF_6^- . Inset: (a) schematic diagram of P3HT chemical structure, and (b) energy-band diagram with bipolaron and allowed optical transitions.

PT and the P3AT's as "pseudopolyenes" with charge-conjugation symmetry is a reasonable first approximation.

Poly(3-hexylthienylene), P3HT, was synthesized as one of the PT derivatives which is soluble in common organic solvents. Although the delocalized electronic structures of conjugated polymers tend to give rise to relatively stiff chains with strong interchain attractive interactions, solubility (and even melting) can be achieved through addition of appropriate side groups. Because of this solubility, P3HT can be prepared in the form of chemically pure films with well-controlled and uniform thickness. In addition to the excellent processibility, P3HT can be doped in solution, thereby enabling uniform doping at a well-defined and accurately reproducible doping level.

In this paper we report a comprehensive (0.05–3 eV) spectroscopic study of poly(3-hexylthienylene) during photoexcitation (i.e., photoinduced absorption) and after doping with NOPF_6 . As with PT and P3MT, we find that charges are predominantly stored in bipolarons. We have observed weak additional features in the photoinduced absorption spectra which we tentatively identify with polaronlike defects, the density of which can be controlled by sample heat-treatment history. Photoinduced-absorption results are also presented for a series of P3HT:PT random copolymers.

II. EXPERIMENTAL TECHNIQUES

The polymers were synthesized by electrochemical polymerization. Detailed sample-purification and -charac-

terization procedures can be found elsewhere.⁸ Thin films of pure P3HT were cast from solution in spectroscopic-grade chloroform onto KBr or sapphire substrates. The thicknesses of the cast films were $\approx 2 \mu\text{m}$ for the infrared measurements (0.05–1 eV) and $\approx 0.2 \mu\text{m}$ for the near-ir and/or visible (0.6–3 eV). After casting onto a substrate, the neutral film was heat-treated at 170°C for 20 h to ensure the completion of the "undoping" process. This high-temperature anneal also serves to minimize structural defects, as discussed in detail in the following section. Chemical doping was carried out in solution; fixed amounts of NOPF_6 dissolved in acetonitrile were added to solutions of P3HT in chloroform with quantities controlled to achieve the desired dopant level. Prior to use, the NOPF_6 was purified by sublimation at 120°C under vacuum and the acetonitrile was dried over calcium hydride. By using the solution-doping technique, we were able to precisely control the uniform doping level.

Copolymers of P3HT with variable fractions of PT were synthesized by random copolymerization (electrochemical) of 3-hexylthiophene and thiophene monomers. The P3HT:PT system was chosen because the clear separation of the C-H out-of-plane vibrations (822 and 788 cm^{-1}) enabled a quantitative characterization of the fraction of PT in the final polymer. Although the oxidation potentials are slightly different, we found that the actual PT concentration determined spectroscopically was in good agreement with the fraction of monomers in the electrolyte solution during polymerization. For insoluble copolymers with high concentrations of PT ($> 75\%$),

semitransparent copolymer-KBr pellets were used for the photoinduced absorption measurements (≈ 0.5 wt. % of copolymer randomly dispersed in KBr).

An IBM Instruments (Bruker) Fourier-transform infrared (FTIR) interferometer, modified to allow access for the external pumping source (Ar⁺ laser), was used to cover the frequency range between 400 cm^{-1} (0.05 eV) and 8000 cm^{-1} (1 eV). Fractional changes in the infrared transmission with the sample at 80 K were measured in response to the external laser incident on the sample for 10 s.⁹ Successive light-on and -off 10-s cycles were signal-averaged until the signal-to-noise ratio was sufficient to obtain the net change in absorption coefficient, $\Delta(\alpha d) = -(\Delta T/T)$, where T is the transmittance, ΔT is the change in transmittance during photoexcitation by the laser pump, and d is the effective sample thickness. Long-time signal averaging was necessary to resolve all the details of the IRAV modes above the noise level (typically 8–48 h). All the doping studies used solution-cast films ($2\text{ }\mu\text{m}$ on KBr substrates and $0.2\text{ }\mu\text{m}$ on sapphire substrates).

Standard photomodulation techniques were used for the photoinduced absorption measurements for frequencies between 0.62 and 2.4 eV (3.0 eV for the doping studies).¹⁰ Again, $-(\Delta T/T)$ was measured to obtain the net change in the absorption coefficient as described above. Since the genuine photoinduced absorption signals are relatively weak, photoluminescence from the sample can contribute to the light incident on the detector in this spectral range. Detailed studies showed that with the narrow collection-angle optics used, the intensity of the photoluminescence was only about 1% of the photoinduced absorption signal due to the photoexcitations.

III. EXPERIMENTAL RESULTS

Doping-induced changes in the absorption coefficient for frequencies between 0.05 and 3.0 eV are shown in Fig. 1. The doping level was 1 mol % of PF₆ per thiophene ring. A number of IRAV modes are observed below 0.25 eV (2000 cm^{-1}), superimposed on the intrinsic infrared modes of the polymer. In addition, two broad electronic transitions (peaked at 0.45 and 1.65 eV, respectively) are observed with associated bleaching beyond the energy gap ($\sim 2.1\text{--}2.2$ eV). Note that these values are slightly different from those of PT [Ref. 2(a)] (0.65 and 1.45 eV) and P3MT [Ref. 2(c)] (0.63 and 1.6 eV), which have been identified as the two subgap states of bipolarons as illustrated in the inset of Fig. 1.

Figure 2 shows the full photoinduced absorption spectrum (pumped with 2.53-eV photons) measured with the sample at 80 K. The spectrum below 0.62 eV was obtained via the steady-state photoinduced absorption technique using the FTIR interferometer and fitted to match the photoinduced-absorption curve (for $\hbar\omega > 0.62$ eV) obtained with the photomodulation technique. A series of photoinduced IRAV modes corresponding to the doping-induced IRAV modes (a more detailed comparison is presented in Fig. 3) were found together with broad electronic transitions peaked at 0.35 and 1.3 eV.

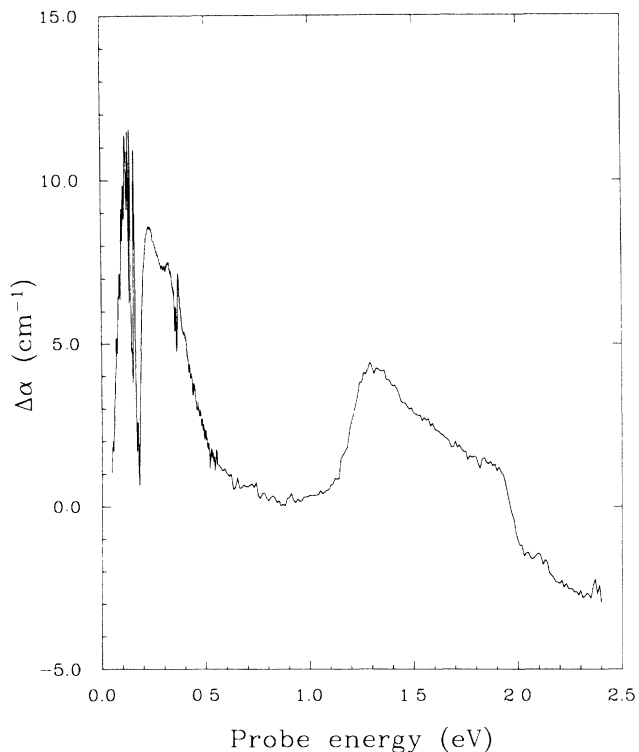


FIG. 2. Photoinduced absorption coefficient of P3HT obtained with 488-nm (2.53-eV) pump energy (50 mW/cm^2) and with the sample at 80 K.

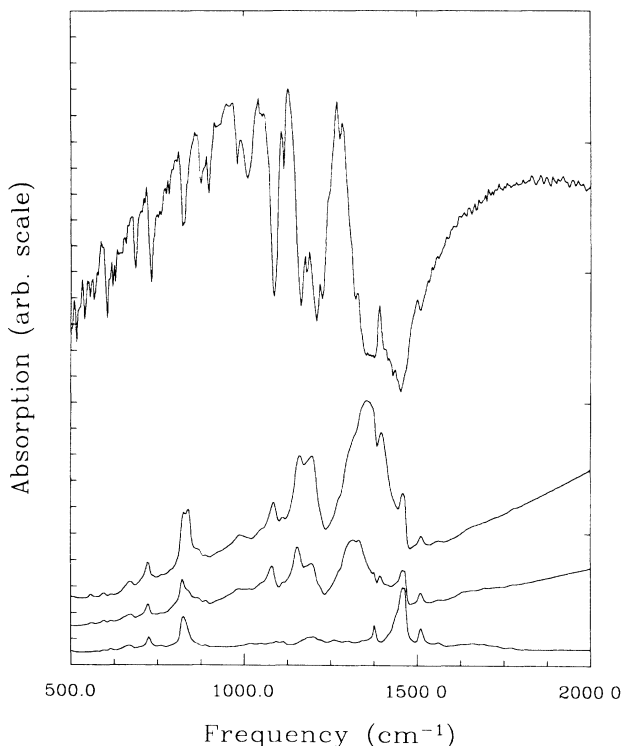


FIG. 3. Detailed photoinduced infrared spectral changes of P3HT (top), and doping-induced infrared spectral changes of P3HT (bottom, undoped; second and third from bottom, 1 and 3 mol % PF₆⁻, respectively).

Notice that there are two relatively strong broad bands at 0.15 eV (with the IRAV modes superimposed) and at 0.21 eV and a weak shoulder at around 1.9 eV.

The IRAV modes obtained through doping and through photoexcitation are compared in detail in Fig. 3. For pure P3HT (the bottom curve in Fig. 3) six characteristic infrared modes are found at 725 cm^{-1} (C—H deformation of methylene group of the hexyl chain) and 822 cm^{-1} (out-of-plane C—H deformation), 1377 cm^{-1} (methyl deformation), and 1454 , 1512 , and 1562 cm^{-1} (ring-stretching modes). Two additional weak features near 1099 (1083) and 1192 (1180) cm^{-1} were observed. The data for two successively higher doping levels (1 and 3 mol %) are shown just above (with baseline offset) for comparison. We identify the doping-induced T modes at 1088 , 1161 , 1200 , and 1354 cm^{-1} , and denote them as T_1 , T_2 , T_3 , and T_4 , respectively, as for PT and P3MT. There are also a number of very weak doping-induced ring-deformation absorption lines, again similar to those observed in PT and P3MT.³ Finally, there is a sharp doping-induced feature on the high-frequency side of T_4 at 1396 cm^{-1} . Since this has no direct correspondence with an additional infrared or Raman line of the pure sample, we assign it as the “third” ir-active weak mode (associated with the nonuniform translation of the bipolaron). This assignment is consistent with the observation of similar features in P3MT at 1388 cm^{-1} and in PT at 1438 cm^{-1} . The photoinduced spectrum (top curve in Fig. 2) shows much sharper features with better definition and better resolution. One sees four T modes at 1041 , 1130 , 1188 , and 1269 cm^{-1} , and the third mode at 1392 cm^{-1} , once again as in PT and P3MT. Presumably the other third modes (one for each T mode) are hidden under the T modes in both the doping-induced and photoinduced spectra.

The 0.15- and 1.9-eV features in the photoinduced spectrum of Fig. 2 have a different physical origin from those of the bipolarons (at 0.35 and 1.3 eV which correspond to the 0.45- and 1.65-eV absorption in the doped films). These features are too weak to show up in the doping-induced spectrum (approximately 10^2 times weaker than the strength of the bipolaron transitions at the 1-mol % doping level), and they decrease substantially upon heat treatment of the sample; this is clearly shown for the 1.9-eV absorption in Fig. 4. We note, furthermore, that the overall magnitude of the photoinduced absorption decreases upon heat treatment, presumably due to more rapid recombination (and a shorter lifetime) as the number of defects is decreased. In addition, we modified the photoinduced-absorption technique to allow longer sampling times in order to resolve the lifetime of the defect-associated absorption at 0.15 eV. We found that the 0.15-eV absorption persists on a time scale of minutes at 80 K, demonstrating that it has a different origin from the electronic transition at 0.3 eV and the photoinduced IRAV modes. We suggest, therefore, that during the film preparation (casting from solution) a relatively small number of defects are introduced which act as deep traps for charge carriers. The additional features which show up in the photoinduced spectrum appear to come from charges associated with such nonintrinsic

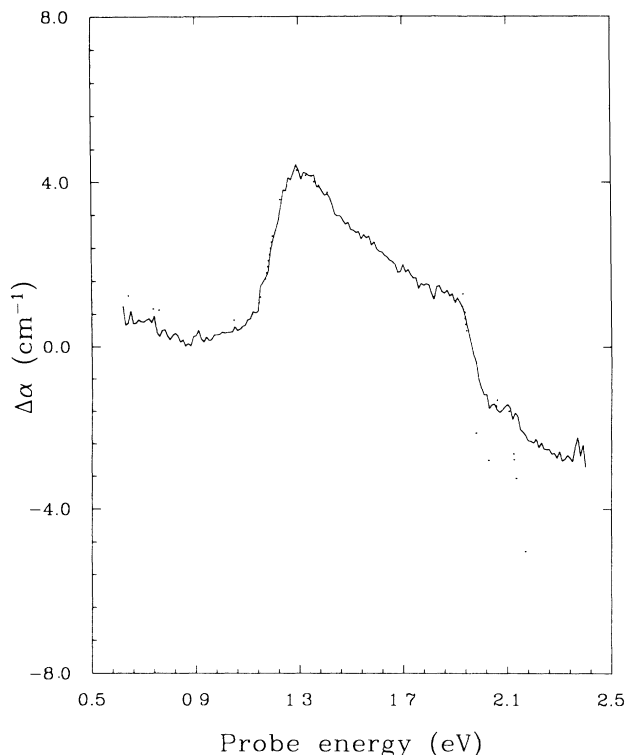


FIG. 4. Change in the photoinduced-absorption spectrum upon heat treatment: dotted curve (before heat treatment) and solid curve (after heat treatment).

trapping sites, the concentration of which can be significantly lowered through thermal annealing. Although the observation of two additional electronic transitions (0.15 and 1.9 eV) is consistent with viewing these as bipolarons with an enhanced confinement parameter, singly charged trapped polaronlike states are not ruled out by the data.

Changes in structural perfection as inferred directly from the relative strength of the 0.15-eV absorption have been monitored as a function of the hexyl side-group concentration as shown in Fig. 5. Starting from 100% PT, one sees the evolution of the photoinduced absorption spectrum to that of P3HT as the fraction of hexyl groups increases. Note, in addition, that the electronic transition is gradually red-shifted by about 0.1 eV and that the shoulder at 0.25 eV (2000 cm^{-1}) increases in oscillator strength with the concentration of hexyl groups. The 0.15-eV absorption starts to show up at the copolymer composition (50% PT)/(50% P3HT), where the material is poorly soluble. The various IRAV modes remain generally the same and can easily be tracked across the entire series.

IV. DISCUSSION

As noted in the Introduction, we can consider PT and P3AT as pseudopolyenes consisting of two *trans* units linked to the next two *trans* units by a *cis* unit, etc. In other words, the confinement energy is expected to be rel-

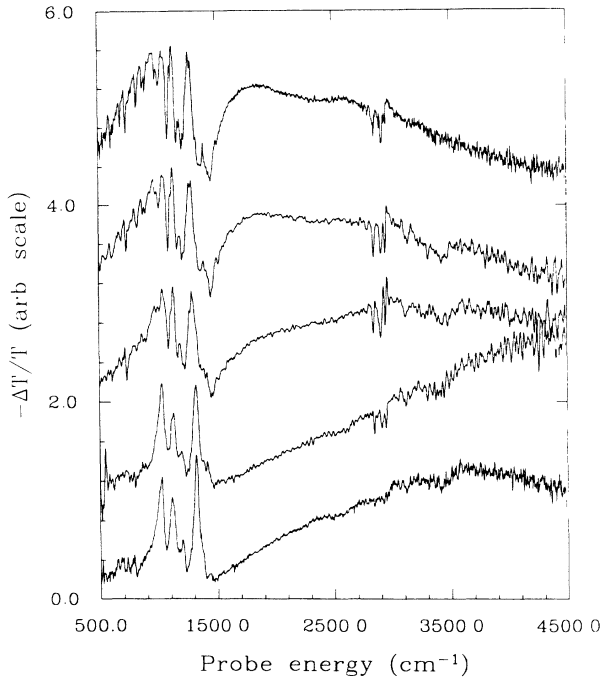


FIG. 5. Detailed changes in the photoinduced activities as a function of hexyl side-group concentration. Starting from 100% PT (bottom), the curves correspond to (75% PT)/(25% P3HT), (50% PT)/(50% P3HT), (25% PT)/(75% P3HT), and 100% P3HT (top).

atively small, comparable to that of $cis-(CH)_x$. The confinement parameter γ is defined as

$$\gamma = \Delta_e / 2\lambda\Delta, \quad (1)$$

where Δ_e is the extrinsic contribution to the energy gap as defined by Brazovskii and Kirova,¹¹ $\Delta = \Delta_e + \Delta_0$ where $\Delta_e = 2\lambda\Delta \ln(\Delta/\Delta_0)$, and λ is the electron-phonon-coupling constant. For $cis-(CH)_x$, γ has been estimated to be in the range 0.5–1.0.¹²

The general features of P3HT as observed in the infrared and visible portions of the spectrum are quite similar to the experimental results reported earlier for PT and P3MT, implying that the charge carriers in P3HT are also bipolarons. One can estimate the confinement parameter γ from the energy difference ($\hbar\omega_0 = \hbar\omega_2 - \hbar\omega_1$) of the doping-induced bipolaron states. As discussed by Fesser *et al.*,¹² γ is determined by the ratio $\hbar\omega_0/\Delta$ where $2\Delta = E_g = \hbar\omega_1$ and $\hbar\omega_2$. In the case of P3HT the observed splitting is $\hbar\omega_0 \approx 1.2$ eV and the energy gap is $2\Delta \approx 2.1$ eV. The implied value for $\hbar\omega_0/\Delta \approx 0.57$ gives $\gamma \sim 0.4$ when compared to the theoretical curve calculated for $cis-(CH)_x$.

The red shift in the photoinduced electronic transitions (as compared with the doping-induced transitions) has been observed in $trans-(CH)_x$, PT, and P3MT. It results from the fact that in photoinduced absorption, for both $\hbar\omega_1$ and $\hbar\omega_2$, the initial state of the bipolaron is doubly charged, whereas the final state is singly charged. Thus

the transition involves a reduction in the Coulomb interaction by an amount U_B . As a result, in the case of photoinduced bipolarons, both transitions are red-shifted by U_B , but their energy difference remains the same. For doping-induced bipolarons, the reduction in Coulomb energy associated with either of the two transitions is approximately canceled by the reduction in the attractive interaction with the charge-neutralizing counterions. We note that for P3HT (as well as for PT and P3MT), $\hbar\omega_0$ is approximately the same for the doping-induced and photoinduced electronic transitions, whereas $\hbar\omega_1 + \hbar\omega_2$ is smaller in the photoinduced spectrum by approximately 0.5 eV; thus, $U_B \approx 0.25$ eV.

When charges are added to the pristine polymer chain by chemical doping or photoexcitation, the IRAV modes appear as a result of the local distortions around the self-localized charged excitations. The resulting infrared conductivity was derived by Horovitz:^{4(a)}

$$\sigma(\omega) = -i\omega(e^2\rho_c/M_d\Omega^2)D_0(\omega)/[1 + (1 - \alpha_p)D_0(\omega)] \quad (2a)$$

where

$$D_0(\omega) = \sum_n (\lambda_n/\lambda)(\omega_n^0)^2/[\omega^2 - (\omega_n^0)^2 - i\omega\delta_n] \quad (2b)$$

is the phonon response function, ω_n^0 are bare phonon frequencies, λ_n is the electron-phonon-coupling constant for the n th mode with $\lambda = \sum_n \lambda_n$, and δ_n is the natural phonon width. The other parameters in Eq. (2a) are as follows: ρ_c is the average charge density, M_d is the dynamic mass of the charged excitation, $\Omega^2 = \sum_n (\lambda_n/\lambda)/(\omega_n^0)^2$, and α_p is the pinning parameter. Since the zeros in the denominator of Eq. (2a) give the infrared absorptions, the pinning parameters for bipolarons in P3HT can be obtained from

$$D_0(\omega) = -1/(1 - \alpha_p). \quad (3)$$

Since resonance Raman data are not available for P3HT, we used the data for the parent PT. A good fit to the observed IRAV frequencies of P3HT with $\alpha_p = 0.21$ for the photoinduced T modes and $\alpha_p = 0.32$ for the doping-induced T modes was achieved. Notice that the size of the pinning parameter for the photoinduced T modes in P3HT is comparable to that of the doping-induced T modes in $trans-(CH)_x$. An estimate of the confinement parameter can be obtained from solving the analogous equation

$$D_0(\omega) = -1/(1 - 2\tilde{\lambda}), \quad (4)$$

where $\tilde{\lambda} = \lambda(1 + \gamma)$. Using the same input parameters, we obtain $\gamma \sim 0.3$, in agreement with the value estimated from the splitting between the two gap states ($\hbar\omega_0$).

Detailed studies of small oscillations around charged excitations based on the SSH model and its continuum version predicted the existence of additional infrared features: the third weak localized mode and weak infrared activity for the extended phonons.⁶ Detailed calculations for $trans-(CH)_x$ by Ito and Ono⁶ are in excellent agreement with the experimental results for charged soli-

tons in polyacetylene.⁷ Similar experimental observations have been made for PT and P3MT, consistent with the predictions of Mele and Hicks (MH).⁵ The MH theory predicts three additional localized modes for bipolarons (only one of which is infrared active) for each of the T modes. In Sec. III, evidence was presented leading to the assignment of the localized mode at 1392 cm^{-1} as an MH mode associated with the highest T mode (the others being unobservable under the more intense overlapping T modes). Although the frequency is in agreement with the MH prediction, the oscillator strength is large compared with that predicted by MH; the source of the discrepancy is not understood.

We propose that there also exists observable extended phonon absorption in the nondegenerate ground-state polymer, as is the case for *trans*-(CH)_x (where the ground state is degenerate). The extra absorption at $\approx 0.25\text{ eV}$ in both the doped and the photoinduced-absorption spectra of P3HT may represent the extended phonon contribution. Similarly, in the spectra for doped and photoexcited P3MT there is a shoulder at about 2200 cm^{-1} (as well as the weak mode at 1384 cm^{-1}). Note that, as shown in Fig. 5, the strength of the extended phonon shoulder grows (in the copolymer series) with the fraction of P3HT.

V. CONCLUSIONS

We have demonstrated through infrared and optical studies of doped and photoexcited poly(3-

hexylthienylene) that bipolarons are the lowest-energy charged excitations in this nondegenerate ground-state system. A one-to-one correspondence between doping-induced and photoinduced spectral features (both phonon and electronic) was observed, consistent with the results for other conducting polymers. We found, however, that minor structural defects are created in P3HT when films are cast from solution. Such defects can be reduced by annealing the polymer at elevated temperatures. As in PT and P3HT, four T modes were observed in P3HT as well as a weak additional bound mode and evidence of extended phonon infrared activity.

From analysis of the photoinduced and doping-induced spectra, we found that change in Coulomb energy between the doubly charged and singly charged bipolaron is $U_B \approx 0.25\text{ eV}$, comparable to that inferred for PT, and significantly less than the $P^\pm + P^\pm \rightarrow B^{2\pm}$ binding energy arising from the electron-phonon interaction. From the splitting between the two gap states, we obtained an estimate of the confinement parameter, $\gamma \sim 0.3\text{--}0.4$. The pinning of the photogenerated bipolarons in P3HT is weaker than in PT, while the pinning of the doping-induced bipolarons is comparable in PT and P3HT.

ACKNOWLEDGMENTS

We thank F. Wudl, Z. Soos, M. Nowak, and N. Colaneri for valuable discussions. This research was supported by the U.S. Office of Naval Research (under Contract No. N0001-83-K0450).

*Permanent address: Central Research Laboratories, Matsushita Electric Industrial Co. Ltd., Moriguchi-shi, Osaka 570, Japan.

¹For a review, see *Handbook of Conducting Polymers*, edited by T. Skotheim (Dekker, New York, 1986).

²(a) T.-C. Chung, J. H. Kaufman, A. J. Heeger, and F. Wudl, *Phys. Rev. B* **30**, 702 (1984); (b) Z. Vardeny, E. Ehrenfreund, O. Brafman, M. Nowak, H. Schaffer, A. J. Heeger, and F. Wudl, *Phys. Rev. Lett.* **56**, 671 (1986); (c) N. Colaneri, M. Nowak, D. Spiegel, S. Hotta, and A. J. Heeger, *Phys. Rev. B* **36**, 7964 (1987).

³(a) H. E. Schaffer and A. J. Heeger, *Solid State Commun.* **59**, 415 (1986); (b) Y. H. Kim, S. Hotta, and A. J. Heeger, *Phys. Rev. B* **36**, 7486 (1976).

⁴(a) B. Horovitz, *Solid State Commun.* **41**, 729 (1982); (b) E. Ehrenfreund, Z. Vardeny, O. Brafman, and B. Horovitz, *Phys. Rev. B* **36**, 1535 (1987).

⁵(a) E. J. Mele and J. C. Hicks, *Phys. Rev. B* **32**, 2703 (1985); (b) A. Terai and Y. Ono, *J. Phys. Soc. Jpn.* **55**, 213 (1986); (c) E. J. Mele and J. C. Hicks, *Synth. Met.* **13**, 149 (1986).

⁶H. Ito and Y. Ono, *J. Phys. Soc. Jpn.* **54**, 1194 (1985).

⁷H. E. Schaffer, R. H. Friend, and A. J. Heeger, *Phys. Rev. B* **36**, 7537 (1987).

⁸S. Hotta, S. D. D. V. Rughooputh, A. J. Heeger, and F. Wudl, *Macromolecules* **20**, 212 (1987).

⁹G. B. Blanchet, C. R. Fincher, T.-C. Chung, and A. J. Heeger, *Phys. Rev. Lett.* **50**, 1938 (1983).

¹⁰N. Colaneri, R. H. Friend, H. E. Schaffer, and A. J. Heeger, *Phys. Rev. B* (to be published).

¹¹S. Brazovskii and N. Kirova, *Pis'ma Zh. Eksp. Teor. Fiz.* **33**, 6 (1981) [*JETP Lett.* **33**, 3 (1981)].

¹²K. Fesser, A. R. Bishop, and D. Campbell, *Phys. Rev. B* **27**, 4804 (1983).